

Fe(II), Ru(II) and Re(I) complexes of endotopic, sterically non-hindering, U-shaped 8,8'-disubstituted-3,3'-biisoquinoline ligands: syntheses and spectroscopic properties†

Barbara Ventura,^{*a} Francesco Barigelletti,^a Fabien Durola,^b Lucia Flamigni,^a Jean-Pierre Sauvage^b and Oliver S. Wenger^b

Received 20th August 2007, Accepted 9th October 2007

First published as an Advance Article on the web 1st November 2007

DOI: 10.1039/b712834g

The redox behaviour, optical-absorption spectra and emission properties of U-shaped and elongated disubstituted biisoquinoline ligands and of derived octahedral Fe(II), Ru(II), and Re(I) complexes are reported. The ligands are 8,8'-dichloro-3,3'-biisoquinoline (**1**), 8,8'-dianisyl-3,3'-biisoquinoline (**2**), and 8,8'-di(phenylanisyl)-3,3'-biisoquinoline (**3**), and the complexes are [Fe(**2**)₃]²⁺, [Fe(**3**)₃]²⁺, [Ru(**1**)(phen)₂]²⁺, [Ru(**2**)₃]²⁺, [Ru(**3**)₃]²⁺, [Re(**2**)(py)(CO)₃]⁺, and [Re(**3**)(py)(CO)₃]⁺. For the ligands, the optical properties as observed in dichloromethane are in line with expectations based on the predominant ¹ππ* nature of the involved excited states, with contributions at lower energies from ¹nπ* and ¹ILCT (intraligand charge transfer) transitions. For all of the Fe(II), Ru(II), and Re(I) complexes, studied in acetonitrile, the transitions associated with the lowest-energy absorption band are of ¹MLCT (metal-to-ligand charge transfer) nature. The emission properties, as observed at room temperature and at 77 K, can be described as follows: (i) the Fe(II) complexes do not emit, either at room temperature or at 77 K; (ii) the room-temperature emission of the Ru(II) complexes ($\phi_{\text{em}} > 10^{-3}$, τ in the μs range) is of mixed ³MLCT/³LC character (and similarly at 77 K); and (iii) the room-temperature emission of the Re(I) complexes ($\phi_{\text{em}} \sim 3 \times 10^{-3}$, $\tau < 1$ ns) is of ³MLCT character and becomes of ³LC (ligand-centered) character (τ in the ms time scale) at 77 K. The interplay of the involved excited states in determining the luminescence output is examined.

Introduction

Bidentate chelates of the 2,2'-bipyridine (bipy) or 1,10-phenanthroline (phen) type play a crucial role as ligands in inorganic photochemistry.¹⁻⁴ Their ruthenium(II), rhenium(I) and, to a lesser extent, osmium(II) and iridium(III) complexes have been extensively used and continue to be much utilised as photo- and electro-active species, in relation to light-energy conversion.⁵⁻⁹ Numerous derivatives of these bidentate chelate archetypes have been prepared and investigated, leading to a wide range of electronic properties for the corresponding ligands and their complexes.¹⁰⁻¹³ As early as 1988, Balzani and his colleagues published a review article in which they gathered the various complexes of this class of compounds.¹⁴ In the same publication, they discuss the properties of hundreds of complexes containing bidentate ligands of the bipy and phen family. Among the many ligands mentioned, 3,3'-biisoquinoline appears as one of the less frequently used bidentate chelates.^{10,15} Since then, a few additional publications dealing with the incorporation of 3,3'-biisoquinoline

chelates in d⁶ transition-metal complexes have appeared but their number is very limited.¹⁶

Recently, we have reported the syntheses and the preliminary structural properties of non-sterically-hindering but endocyclic ligands **1**, **2** and **3**, illustrated in Scheme 1, and their complexes [Fe(**2**)₃]²⁺, [Fe(**3**)₃]²⁺, [Ru(**2**)₃]²⁺, [Re(**2**)(py)(CO)₃]⁺, and [Re(**3**)(py)(CO)₃]⁺.^{17,18} The key building block for such systems is a 3,3'-biisoquinoline, the 8 and 8' positions of which have been functionalised by various aromatic groups. We now report on the syntheses of [Ru(**1**)(phen)₂](PF₆)₂ and [Ru(**3**)₃](PF₆)₂ and on the electrochemical and spectroscopic properties in acetonitrile of the series of Fe(II), Ru(II) and Re(I) complexes; a similar characterization of the ligands has been carried out in dichloromethane for comparison purposes.

Experimental

Syntheses

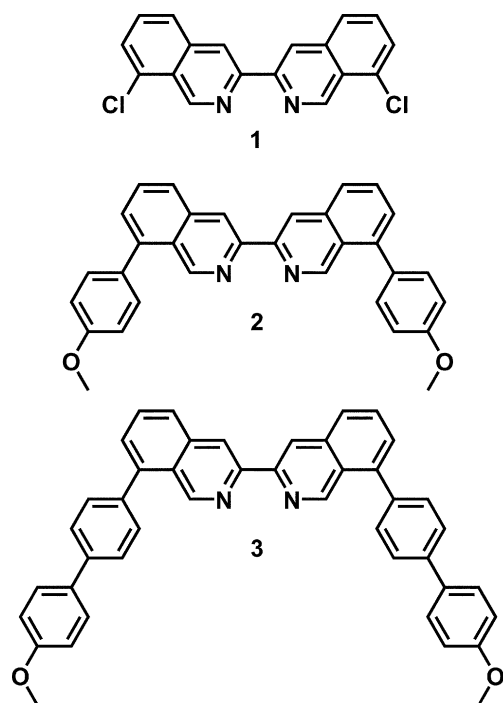
The following chemicals were obtained commercially and were used without further purification: trifluoromethanesulfonic anhydride (Acros), [1,2-bis(diphenylphosphino)ethane]dichloronickel(II) (Aldrich), trifluoroacetic acid (Aldrich).

¹H and ¹³C NMR spectra were recorded with a Bruker AVANCE 300 [300 MHz (¹H); 75 MHz (¹³C)] spectrometer, using deuterated solvent as the lock. The spectra were collected at 25 °C and the chemical shifts were referenced to residual

^aIstituto per la Sintesi Organica e la Fotoreattività (ISOF), Consiglio Nazionale delle Ricerche (CNR), Via P. Gobetti 101, 40129, Bologna, Italy. E-mail: bventura@isof.cnr.it

^bLaboratoire de Chimie Organo-Minérale, LC3 du CNRS, Institut de Chimie, Université Louis Pasteur, 4 rue Blaise Pascal, 67070, Strasbourg Cedex, France

† Electronic supplementary information (ESI) available: Experimental details of the synthesis of **4**, **6** and **7**. See DOI: 10.1039/b712834g



Scheme 1 Schematic structures of ligands.

solvent protons as internal standards. ^1H : CDCl_3 7.27 ppm, CD_2Cl_2 5.32 ppm, CD_3CN 1.96 ppm, DMSO-d_6 2.50 ppm. Mass spectra were obtained with a VG ZAB-HF spectrometer (FAB) and a VG-BIOQ triple quadrupole in positive or negative mode (ES-MS).

All silica-column chromatographies were performed using Merck Silicagel 60 (0.063–0.200 mm).

Electrochemical measurements were performed with a three-electrode system consisting of a platinum working electrode, a platinum wire-counter electrode, and a silver wire as a pseudo-reference electrode (ferrocene was then used as a reference). All measurements were carried out under Ar, in degassed spectroscopic-grade acetonitrile, using 0.1 M *n*- Bu_4NBF_4 solutions as supporting electrolyte. An EG&G Princeton Applied Research model 273A potentiostat connected to a computer was used (software from Princeton Applied Research).

8-Chloroisoquinolin-3-yl trifluoromethanesulfonate. A solution of 8-chloroisoquinolin-3-ol (1.04 g, 5.8 mmol) in dry pyridine (40 mL) was cooled to 0 °C and carefully treated with trifluoromethanesulfonic anhydride (1.6 mL, 2.7 g, 9.2 mmol). The mixture was allowed to warm to room temperature and stirred over night. The solvent was removed under reduced pressure. The crude product was purified by chromatography on silica gel by using pentane–diethyl ether (1 : 4) as the eluent to afford the title product (colourless crystals, 1.71 g, 95%). ^1H NMR (CD_2Cl_2 , 300 MHz): δ = 9.52 (s, 1H), 7.93–7.89 (m, 1H), 7.80–7.76 (m, 2H), 7.67 (s, 1H). ES-MS m/z = 312.1150 (calculated 311.9709 for $\text{C}_{10}\text{H}_5\text{ClF}_3\text{NO}_3\text{S} + \text{H}^+$).

8,8'-Dichloro-3,3'-biisoquinoline 1. Zinc powder was activated by treatment of 20 g in 100 mL of acetic acid for 1 hour. After filtration, the powder was washed three times with distilled water and dried under vacuum for 6 hours at 120 °C. Dichloro[1,2-bis(diphenylphosphino)ethane]nickel(II) (32 mg, 0.06 mmol), zinc

powder (0.4 g, 6.1 mmol), potassium bromide (280 mg, 2.4 mmol) and 8-chloroisoquinolin-3-yl trifluoromethanesulfonate (200 mg, 0.64 mmol) were stirred in 5 mL of dry and degassed THF for 5 hours at 70 °C. The solvent was evaporated and the residue dissolved in dichloromethane (10 mL), distilled water (10 mL) and a 32% ammonium hydroxide solution (1 mL). The organic phase was separated and the aqueous phase extracted twice with dichloromethane. The combined organic phases were washed once with distilled water and then evaporated. The crude product was purified by chromatography on silica gel by using dichloromethane–methanol (98 : 2) as the eluent to give the title compound (white solid, 26 mg, 25%). ^1H NMR (CDCl_3 , 300 MHz): δ = 9.77 (s, 2H), 8.95 (s, 2H), 7.94–7.91 (m, 2H), 7.66–7.73 (m, 4H). ES-MS m/z = 325.0373 (calculated 325.0299 for $\text{C}_{18}\text{H}_{10}\text{Cl}_2\text{N}_2 + \text{H}^+$).

[Ru(1)(phen)] $_2$ (PF $_6$) $_2$. 17 mg (0.020 mmol) of $[\text{Ru}(\text{phen})_2(\text{MeCN})_2](\text{PF}_6)_2$ and 7.0 mg (0.022 mmol) of 8,8'-dichloro-3,3'-biisoquinoline **1** were dissolved in 2 mL of ethylene glycol. The solution was heated to 140 °C under argon for 3 hours and then allowed to cool to room temperature. The crude product was precipitated by addition of a saturated aqueous solution of potassium hexafluorophosphate and cold distilled water. The orange precipitate was purified by column chromatography (silica; eluent: acetone, water, saturated aqueous solution of potassium nitrate, 80 : 5 : 0.5 (v/v/v); re-precipitation with a saturated aqueous solution of potassium hexafluorophosphate in water). This procedure yielded 20 mg (0.019 mmol; 91%) of pure $[\text{Ru}(\mathbf{1})(\text{phen})_2](\text{PF}_6)_2$ as an orange powder. ^1H NMR (CD_2Cl_2 , 300 MHz): δ = 9.50 (s, 2H), 8.90–8.80 (m, 6H), 8.65 (s, 2H), 8.55 (dd, 2H, J = 5.1, 1.2 Hz), 8.45 (dd, 4H, J = 10.2, 8.7 Hz), 8.23 (d, 2H, J = 8.1 Hz), 7.93–7.80 (m, 8H). EM-MS m/z = 931.07 (calculated 931.03 for $\text{C}_{42}\text{H}_{26}\text{Cl}_2\text{F}_6\text{N}_6\text{PRu}^+$).

[Ru(3)] $_3$ (PF $_6$) $_2$. 211 mg (0.340 mmol) of 8,8'-di(phenylanisyl)-3,3'-biisoquinoline were suspended in 300 mL of 1,2-dichloroethane. With the addition of 0.5 mL trifluoroacetic acid this mixture turned into a yellow homogenous solution. After adding 49 mg (0.100 mmol) of ruthenium(II) tetra(dimethylsulfoxide) dichloride the solution was refluxed under argon for 24 hours whereby it turned deep red. Then the solvent was evaporated, the residue was taken up in tetrahydrofuran, and the crude product was precipitated by addition of a saturated aqueous solution of potassium hexafluorophosphate. The orange precipitate was purified by column chromatography (silica; eluent: acetonitrile, water, saturated aqueous solution of potassium nitrate, 200 : 10 : 1 (v/v/v); re-precipitation with a saturated aqueous solution of potassium hexafluorophosphate in water). This procedure yielded 130 mg (0.058 mmol; 58%) of pure $[\text{Ru}(\mathbf{3})_3](\text{PF}_6)_2$ as an orange powder. ^1H NMR (CD_3CN): δ = 8.88 (s, 6H; H^1), 8.35 (s, 6H; H^4), 7.75 (d, 6H, J = 8.1 Hz; H^7), 7.27 (d, 12H, J = 8.7 Hz), 7.20–7.02 (m, 36H), 6.79 (d, 12H, J = 8.1 Hz), 3.91 (s, 18H, OCH_3). ES-MS m/z = 981.3194 (calculated 981.3230 for $\text{C}_{132}\text{H}_{96}\text{N}_6\text{O}_6\text{Ru}^{2+}$).

Optical spectroscopy

Spectrophotometric-grade dichloromethane and acetonitrile at 295 K and at 77 K were used without further purification. Absorption spectra of dilute solutions (2×10^{-5} M) in dichloromethane (for the ligands) and acetonitrile (for the complexes) were

obtained with a Perkin-Elmer Lambda 45 UV-vis spectrometer. For luminescence experiments, the samples were placed in fluorimetric 1-cm-path cuvettes and purged of oxygen by bubbling with argon or by evacuating with repeated freeze–pump–thaw cycles. Uncorrected luminescence spectra were obtained with a Spex Fluorolog II spectrofluorimeter equipped with a Hamamatsu R928 phototube. Sample solutions were excited at the indicated wavelength (see below), and dilution was adjusted to obtain absorbance values ≤ 0.15 . While uncorrected luminescence-band maxima are used throughout the text, corrected spectra were employed for the determination of the luminescence quantum yields. The correction procedure is based on the use of software which takes care of the wavelength-dependent phototube response. From the wavelength-integrated area of the corrected luminescence spectra we obtained luminescence quantum yields ϕ_{em} with reference to a standard with known yield, ϕ_r , and by using eqn (1):¹⁹

$$\frac{\phi_{em}}{\phi_r} = \frac{Abs_r \cdot \eta^2 \cdot (area)}{Abs \cdot \eta_r^2 \cdot (area)} \quad (1)$$

where Abs and η are the absorbance values and refractive index of the solvent respectively. For the ligands λ_{exc} was 330 nm and the reference was quinine sulfate in aerated 1 N sulfuric acid, $\phi_r = 0.546$.²⁰ For the Fe(II) and Ru(II) complexes, λ_{exc} was 450 nm; for the Re(I) complexes λ_{exc} was 390 nm; for both cases the reference was $[Ru(bpy)_3]Cl_2$ in air-equilibrated water, $\phi_r = 0.028$.²¹ Band maxima and relative luminescence intensities were affected by an uncertainty of 2 nm and 20% respectively. Luminescence lifetimes were obtained by using an IBH 5000 F single-photon counting spectrometer. Excitation was performed by using nanoLED sources at 331 nm for the ligands, and 465 and 373 nm for the Ru(II) and Re(I) complexes respectively. The Fe(II) complexes did not show any emission. Analysis of the luminescence-decay profiles against time was accomplished by using software provided by the manufacturers. EHMO calculations were performed on the ligands with standard programs from the CS ChemOffice package, Cambridge Corporation, MA; the geometry of the ligands was optimized by using a MM2 approach, with the chelating rings kept parallel to simulate the coordination arrangement.

Results and discussion

Syntheses and characterization

The synthetic route leading to bisisoquinoline **1** is represented in Scheme 2. Isoquinoline **7**, functionalized on its 3 and 8 positions, is synthesized following an existing methodology:²² sodium diethoxy acetate **4** is first activated with thionyl chloride and subsequently condensed with 2-chlorobenzylamine **5** in 59% yield. The resulting amide **6** cyclizes in concentrated sulfuric acid to form 8-chloroisoquinolin-3-ol **7** in a so-called Pomeranz–Fritsch reaction (71% yield). Activation of its alcohol function using triflic anhydride results in the formation of triflate compound **8** in nearly quantitative yield (95%). Ligand **1** is then obtained in 25% yield by a nickel-catalyzed homocoupling reaction between two triflate molecules **8**. In addition to the relatively poor yield of this last step, the purification of **1** is difficult because of its very low solubility, which is why the global strategy for synthesis of functionalized bisisoquinolines has been revised.

In spite of the small amount of **1** that was obtained, one heteroleptic complex of ruthenium, $[Ru(\mathbf{1})(phen)_2]^{2+}$, has been synthesised from $[Ru(MeCN)_2(phen)_2]^{2+}$ with a very good yield (91%).

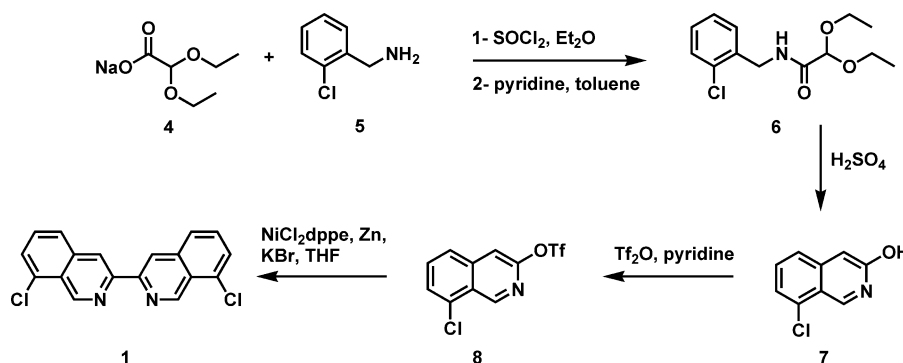
Ligands **2** and **3** have been described in previous papers¹⁶ as well as their Fe(II), Re(I) complexes and the homoleptic $[Ru(\mathbf{2})_3]^{2+}$ complex.^{16–18} $[Ru(\mathbf{3})_3]^{2+}$ has been obtained in a relatively different way than $[Ru(\mathbf{2})_3]^{2+}$ because of the poor solubility of **3**. In this case, addition of an acid is necessary to solubilize the ligand, and complexation is then possible thanks to the better association constant of the complex.

Electrochemistry

The obtained oxidation potentials $E_{1/2}^{ox}$ for the complexes are collected in Table 1, and are discussed below in connection with the spectroscopic properties. The solubility of $[Ru(\mathbf{3})_3](PF_6)_2$ in MeCN is about 1 mg in 5 mL (about 5 mg in 5 mL for the other complexes), and, due to the low solubility, the value given in the table should be taken with some care.

Absorption spectra

The absorption spectra of ligands **1**, **2**, and **3** in dichloromethane are shown in Fig. 1, and absorption data are listed in Table 2. The high-intensity bands peaking below 300 nm ($\epsilon \sim 5 \times 10^4 \text{ M}^{-1} \text{ s}^{-1}$)

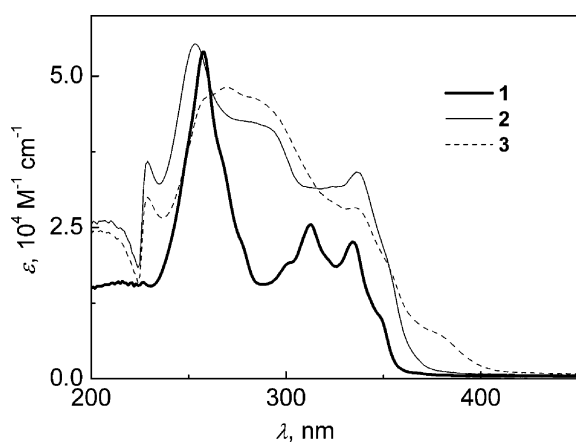


Scheme 2 The synthesis of **4**, **6**, and **7** is outlined in the ESI.†

Table 1 Half-wave oxidation potentials of the Fe(II), Ru(II) and Re(I) complexes^a

| | $E_{1/2}^{ox}/V$ vs. SCE |
|--|--------------------------|
| [Fe(2) ₃] ²⁺ | +1.01 |
| [Fe(3) ₃] ²⁺ | +1.00 |
| [Ru(1)(phen) ₂] ²⁺ | +1.32 |
| [Ru(2) ₃] ²⁺ | +1.18 |
| [Ru(3) ₃] ²⁺ | (+1.62) ^b |
| [Re(2)(py)(CO) ₃] ⁺ | +1.93 |
| [Re(3)(py)(CO) ₃] ⁺ | +1.75 |

^a In degassed acetonitrile, using 0.1 M *n*-Bu₄NBF₄ solutions as supporting electrolyte. ^b Value affected by a high uncertainty due to the poor solubility of the complex.

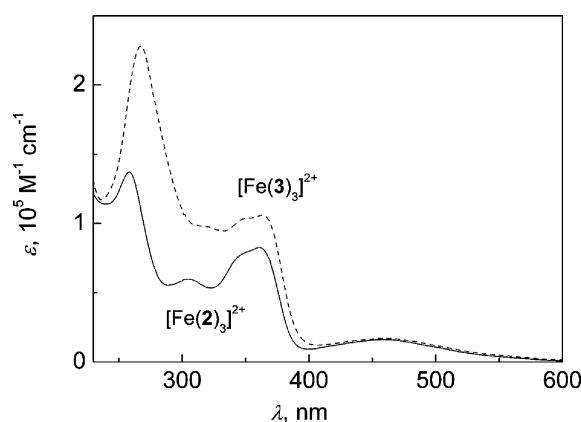
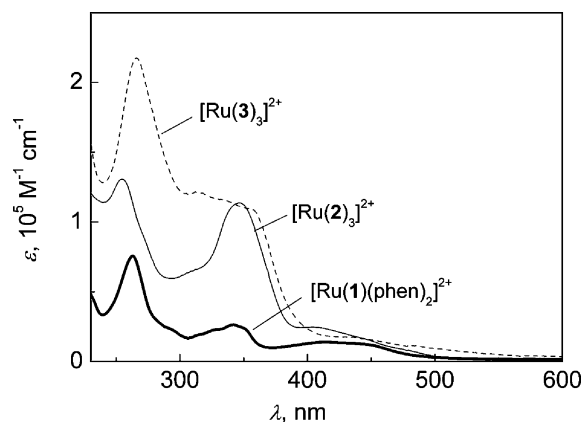
**Fig. 1** Absorption spectra of ligands **1** (thick solid line), **2** (thin solid line) and **3** (dashed line) in dichloromethane at room temperature.**Table 2** Absorption data^a

| | λ_{max}/nm | $\epsilon/(10^5 M^{-1} cm^{-1})$ |
|--|--------------------|----------------------------------|
| 1 | 258 | 0.54 |
| | 334 | 0.23 |
| 2 | 253 | 0.55 |
| | 336 | 0.34 |
| 3 | 269 | 0.48 |
| | 336 | 0.28 |
| [Fe(2) ₃] ²⁺ | 378 | 0.07 (sh) |
| | 258 | 1.37 |
| | 361 | 0.83 |
| [Fe(3) ₃] ²⁺ | 458 | 0.16 |
| | 267 | 2.28 |
| | 364 | 1.06 |
| [Ru(1)(phen) ₂] ²⁺ | 458 | 0.17 |
| | 263 | 0.76 |
| | 342 | 0.26 |
| [Ru(2) ₃] ²⁺ | 413 | 0.14 |
| | 255 | 1.31 |
| | 347 | 1.14 |
| [Ru(3) ₃] ²⁺ | 405 | 0.25 |
| | 266 | 2.18 |
| | 357 | 1.09 (sh) |
| [Re(2)(py)(CO) ₃] ⁺ | 433 | 0.18 |
| | 259 | 0.36 |
| | 391 | 0.14 |
| [Re(3)(py)(CO) ₃] ⁺ | 268 | 0.66 |
| | 390 | 0.24 |

^a In dichloromethane solvent for the ligands and acetonitrile for the complexes, at room temperature.

are ascribed to allowed ¹ππ* transitions, while for the region 300–400 nm transitions of different character overlap.^{23,24} In this region, contributions from both weaker ¹nπ* and intraligand charge transfer (¹ILCT) transitions might be expected, the latter due also to the presence of electron-releasing (methoxy) and electron-accepting (chloride) subunits interacting with the bisquinoline ligand frame. The spectra appear reasonably homogeneous within the series, except for a progressive extension of the absorption tail in the range 350–400 nm on passing from **1** to **3**. This is ascribable to the elongation of the peripheral arms of the bisquinoline unit, which leads to an increased delocalisation of the π orbitals and a smaller HOMO–LUMO gap (see below for a discussion on this point).

The absorption spectra of the examined Fe(II), Ru(II) and Re(I) complexes in acetonitrile are displayed in Fig. 2–4 respectively. Absorption data are collected in Table 2. For discussing the general features of the absorption spectra of the complexes, one may take into account the spectral portions below and above 400 nm, as dealt with in the following.

**Fig. 2** Absorption spectra of complexes [Fe(2)₃]²⁺ (thin solid line) and [Fe(3)₃]²⁺ (dashed line) in acetonitrile at room temperature.**Fig. 3** Absorption spectra of complexes [Ru(1)(phen)₂]²⁺ (thick solid line), [Ru(2)₃]²⁺ (thin solid line) and [Ru(3)₃]²⁺ (dashed line) in acetonitrile at room temperature.

(i) For the Fe(II)^{25,26} and Ru(II)¹⁴ complexes, the bands below 400 nm can be ascribed to transitions mainly centered on the ligands, which likely include ¹LC and ¹ILCT transitions, as

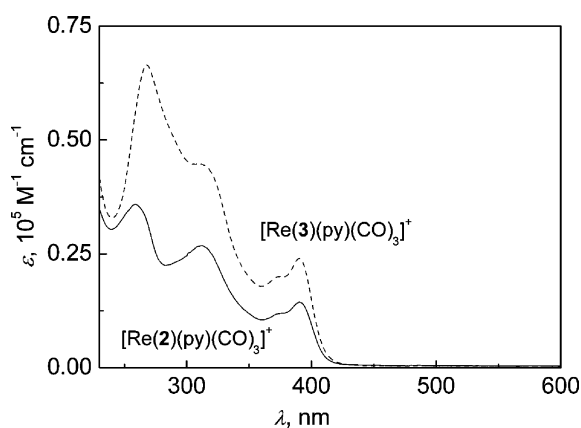


Fig. 4 Absorption spectra of complexes $[\text{Re}(\mathbf{2})(\text{py})(\text{CO})_3]^+$ (thin solid line) and $[\text{Re}(\mathbf{3})(\text{py})(\text{CO})_3]^+$ (dashed line) in acetonitrile at room temperature.

mentioned above. These exhibit a bathochromic shift with respect to the case of corresponding ligands, as suggested by comparison of Fig. 1 and 2. This is likely a consequence of the stabilization of the orbitals of the ligand upon coordination to a positive metal ion, in turn leading to a reduced energy gap between HOMO and LUMO orbitals. The perturbation effect of the metal centre on the electronic transitions of the ligands can further account for the observed changes in the extinction coefficient (ϵ , Table 2). For the Re(I) complexes,²⁷ the same line of reasoning seems to hold, however, the LC-absorption region is somewhat confined to higher energy, *i.e.* below 350 nm. The MLCT (metal-to-ligand charge transfer) absorption transitions fall in the 350 to 400 nm region, in agreement with previously reported cases.^{28,29} This is due to the presence of the electron-withdrawing CO groups which render the metal centre more electron-deficient than its formal +1 charge.

(ii) For the Fe(II) and Ru(II) complexes studied here, the band systems in the region 400–600 nm can be assigned to ¹MLCT transitions, in agreement with previous reports on related complexes.^{14,25} In particular, the ¹MLCT peak is found at 458 nm for the Fe(II) complexes and in the 405 to 433 nm range for the Ru(II) complexes, with extinction coefficients, $\epsilon \sim 2 \pm 1 \times 10^4 \text{ M}^{-1} \text{ cm}^{-1}$, in line with expectation for ¹MLCT transitions. With regard to the latter complexes, it is interesting to recall the behaviour of a previously investigated series of heteroleptic species, $[\text{Ru}(\text{bpy})_n(\text{i-biq})_{3-n}]^{2+}$, with $n = 1, 2, 3$, and where i-biq is 3,3'-biisoquinoline.^{10,15} In that series, the lowest-energy absorption peak is at 452 nm for $[\text{Ru}(\text{bpy})_3]^{2+}$, 392 nm for $[\text{Ru}(\text{i-biq})_3]^{2+}$ and at intermediate positions for the intermediate cases, $[\text{Ru}(\text{bpy})_2(\text{i-biq})]^{2+}$ and $[\text{Ru}(\text{bpy})(\text{i-biq})_2]^{2+}$. This was explained by admitting that $\text{Ru} \rightarrow \text{bpy}$ CT (charge transfer) states are lower in energy than the corresponding $\text{Ru} \rightarrow \text{i-biq}$ CT levels. Given the close similarity of bpy and phen ligands,¹⁴ these findings suggest that for $[\text{Ru}(\mathbf{1})(\text{phen})_2]^{2+}$ the lowest-lying ¹MLCT transitions, $\lambda_{\text{max}} = 413 \text{ nm}$ (Table 2), could involve the phen ligand and not ligand **1**. Consistent with this, for $[\text{Ru}(\mathbf{2})_3]^{2+}$ and $[\text{Ru}(\mathbf{3})_3]^{2+}$ the lowest-lying ¹MLCT band likewise appears blue-shifted (Table 2) with respect to the case of $[\text{Ru}(\text{phen})_3]^{2+}$, $\lambda_{\text{max}} = 477 \text{ nm}$.¹⁴

It is interesting to notice that for the series of biisoquinoline ligands **1**, **2**, and **3**, the increased size is expected to result in a significant stabilization of the LUMO orbital (the accepting

orbital for a $\text{M} \rightarrow \text{L}$ CT transition), with respect to what happens for the phen ligand. Results from EHMO (Extended Hückel Molecular Orbitals) calculations are summarized in Fig. 5, where for comparison purposes the cases of bpy and i-biq are also given; the bottom plot reports the estimated LUMO levels. The fact that for $[\text{Ru}(\mathbf{2})_3]^{2+}$, and $[\text{Ru}(\mathbf{3})_3]^{2+}$ the lowest-lying ¹MLCT band is blue-shifted with respect to what happens for $[\text{Ru}(\text{phen})_3]^{2+}$ is apparently in contrast with the predictions based on the trend for the ligand LUMO levels. This discrepancy might be a consequence of a complex balance of electrostatic factors that could not be investigated in detail because we were unable to observe the ligand-based reduction processes. With regard to the metal-based oxidation potentials $E_{1/2}^{\text{ox}}$ (Table 1), these appear consistent with the absorption properties discussed above. For instance, for the series $[\text{Fe}(\mathbf{2})_3]^{2+}$, $[\text{Ru}(\mathbf{2})_3]^{2+}$, and $[\text{Re}(\mathbf{2})(\text{py})(\text{CO})_3]^+$, $E_{1/2}^{\text{ox}} = +1.01, +1.18, \text{ and } +1.93 \text{ V}$ respectively (*vs.* SCE). For this series, therefore, given the metal-to-ligand CT nature of the transitions in the lowest-energy region, and by noticing that the same ligand **2** is involved, a correlation between $E_{1/2}^{\text{ox}}$ values and the energy of the ¹MLCT transitions is expected and found to (qualitatively) hold, λ_{max} being 458, 405, and 391 nm (Table 2) respectively.

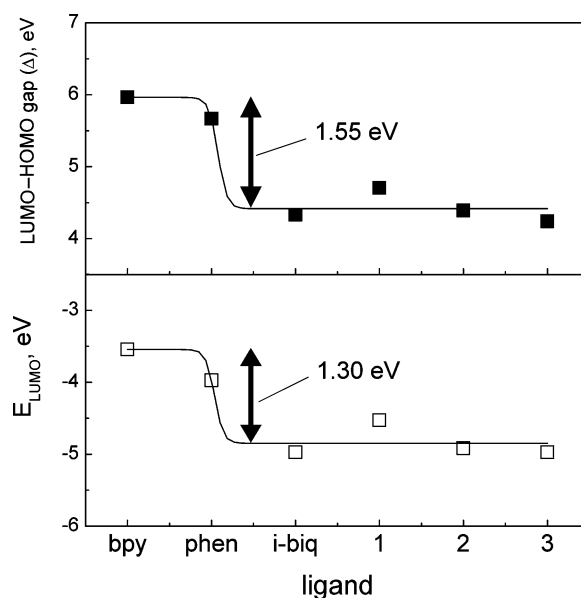


Fig. 5 Results of EHMO calculations for the indicated ligands with a planar arrangement of the chelating subunits. Bottom panel, LUMO level; top panel, LUMO–HOMO gap.

The results from EHMO calculations provide another useful indication. As illustrated in the top panel of Fig. 5, the HOMO–LUMO gap (Δ) for i-biq, **1**, **2**, and **3** is smaller than for the cases of bpy and phen ($\Delta = 1.55 \text{ vs. } 2.6 \text{ eV}$ respectively). Along the same series of ligands, the LUMO orbital (the one bound to play as accepting site for the promoted electron during the MLCT transition) undergoes a smaller stabilization, by *ca.* 1.30 eV. According to these results, the LC excited levels for i-biq, **1**, **2**, and **3** might be expected to be low enough in energy to approach the corresponding MLCT levels, an occurrence that could result in a mixed LC/MLCT character for the emission of the complexes (see below).

Luminescence and photophysics

The luminescence properties of ligands **1**, **2**, and **3** in aerated dichloromethane both at room temperature and at 77 K are reported in Table 3 and illustrated in Fig. 6. For these ligands, the room-temperature emission spectra can reasonably be assigned to the lowest singlet level.³⁰ At this temperature, a bathochromic shift is registered on passing from **1** to **3**, the latter presenting a tail extending up to 600 nm. This trend is in accordance with the observed broadening of the absorption spectra toward low energies. Lifetimes of the order of 3–4 ns (Table 3) and quite

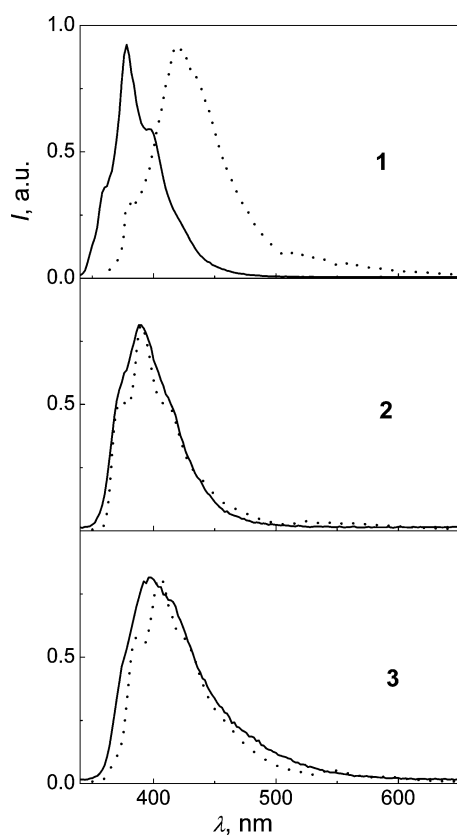


Fig. 6 Arbitrarily scaled luminescence spectra of ligands **1** (top), **2** (middle) and **3** (bottom) in dichloromethane at room temperature (solid line) and at 77 K (dotted line). Excitation at 330 nm.

high fluorescence quantum yields (0.11–0.56) are in agreement with values observed for similar compounds.³⁰ It is interesting to note that along the **1**, **2**, **3** series an increase of the fluorescence quantum yield is observed (Table 3). Since **3** also presents the smallest lifetime in the ligand series, $\tau = 2.8$ ns, its radiative rate constant ($k_r = \phi_{em}/\tau$) is rather high, $k_r = 2 \times 10^8$ s⁻¹.³¹

The 77 K fluorescence spectra of ligands **1** and **3** are red-shifted compared to the room-temperature cases, as expected for ¹LC emission of predominantly $\pi\pi^*$ character,³¹ whereas for ligand **2**, emission peaks are found to be practically coincident. Ligand **1** fluorescence shows the largest red-shift (42 nm) on passing from fluid to rigid solvent whereas for **3** a smaller bathochromic shift (9 nm) is found (Fig. 6 and Table 3). No phosphorescence could be detected for **1**, **2**, and **3**. Ligand **1** differs from the other two ligands also because its lifetime increases from 4.0 to 11.0 ns in passing from room temperature to 77 K, whereas for ligands **2** and **3** the lifetimes appear almost identical at the two temperatures (Table 3). This peculiar behaviour can most likely be related to a smaller rotational freedom in the glass for the bulkier **2** and **3** ligands as compared to **1**. Actually, free rotation about the central C–C single bond can presumably affect the excited-state deactivation. This could account for the low fluorescence quantum yield of **1** at room temperature as compared to **2** and **3** (Table 3). Accordingly, the fluorescence intensity of **1** becomes strongly enhanced in the frozen solvent (about three times, according to what is suggested by the lifetimes), whereas ligands **2** and **3**, already strong emitters at room temperature ($\phi_{em} = 0.39$ and 0.56 respectively, Table 3), are less sensitive to the rigidification effect.

No luminescence can be registered for $[\text{Fe}(\mathbf{2})_3]^{2+}$ and $[\text{Fe}(\mathbf{3})_3]^{2+}$, either at room temperature or at 77 K. This is due to the fact that the lowest-lying excited levels for polyimine complexes of the Fe(II) centre are non-emissive, being of MC (metal-centered) nature, with the ³MLCT levels lying higher in energy, as is well documented in the literature.²⁵

The Ru(II) and Re(I) complexes studied here exhibit weak triplet luminescence features, with room-temperature luminescence quantum yields falling in the range 7.5×10^{-3} – 3×10^{-4} . A summary of their luminescence properties is reported in Table 3 and the spectra are displayed in Fig. 7 and 8. We examine first the simpler case, that of the Re(I) metal centre.

For the Re(I) complexes, the presence of the electron-withdrawing CO groups renders the metal centre more

Table 3 Luminescence properties of ligands and Ru(II) and Re(I) complexes^a

| | 298 K | | | 77 K | |
|--|----------------------------|-----------------|------------------|----------------------------|-------------------|
| | λ_{em}/nm^b | ϕ_{em}^c | τ/ns | λ_{em}/nm^b | τ/ns |
| 1 ^d | 378 | 0.11 | 4.0 | 420 | 11.0 |
| 2 ^d | 389 | 0.39 | 4.2 | 390 | 4.2 |
| 3 ^d | 397 | 0.56 | 2.8 | 406 | 2.9 |
| $[\text{Ru}(\mathbf{1})(\text{phen})_2]^{2+},^e$ | 586 | 0.0075 (0.0034) | 260 (80) | 581 | 5.2×10^3 |
| $[\text{Ru}(\mathbf{2})_3]^{2+},^e$ | 566 | 0.0027 (0.0005) | 920 (120) | 581 | 5.1×10^3 |
| $[\text{Ru}(\mathbf{3})_3]^{2+},^e$ | 566 | 0.0018 (0.0004) | 870 (130) | 581 | 4.6×10^3 |
| $[\text{Re}(\mathbf{2})(\text{py})(\text{CO})_3]^+,^f$ | 470 | 0.0003 | <0.5 | 572 | 1.5×10^6 |
| $[\text{Re}(\mathbf{3})(\text{py})(\text{CO})_3]^+,^f$ | 530 | 0.0029 | <0.5 | 577 | 1.6×10^6 |

^a In degassed dichloromethane solvent for the ligands and acetonitrile for the complexes; within brackets, values for air-equilibrated solvents. ^b Emission maxima. ^c Luminescence quantum yields. ^d Excitation at 330 and 331 nm for the luminescence spectra and lifetime determinations respectively. ^e Excitation at 450 and 465 nm for the luminescence spectra and lifetime determinations respectively. ^f Excitation at 410 and 373 nm for the luminescence spectra and lifetime determinations respectively.

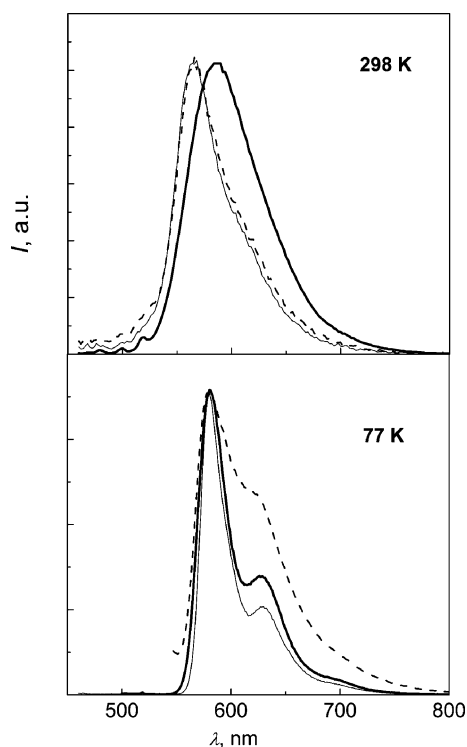


Fig. 7 Arbitrarily scaled luminescence spectra of complexes $[\text{Ru}(\text{1})(\text{phen})_2]^{2+}$ (thick solid line), $[\text{Ru}(\text{2})_3]^{2+}$ (thin solid line) and $[\text{Ru}(\text{3})_3]^{2+}$ (dashed line) in acetonitrile at room temperature (top) and 77 K (bottom). Excitation at 450 nm.

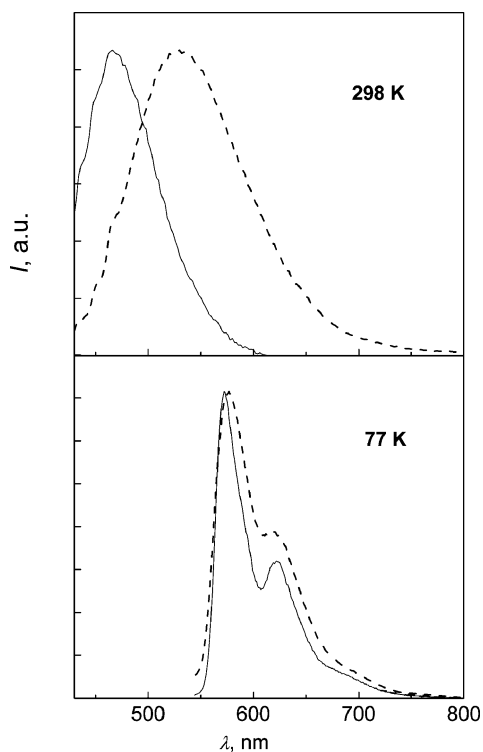


Fig. 8 Arbitrarily scaled luminescence spectra of complexes $[\text{Re}(\text{2})(\text{py})(\text{CO})_3]^+$ (solid line), and $[\text{Re}(\text{3})(\text{py})(\text{CO})_3]^+$ (dashed line) in acetonitrile at room temperature (top) and 77 K (bottom). Excitation at 390 nm.

electron-deficient than its formal +1 charge, as also suggested by the high values for the oxidation step (Table 1).^{27–29} The room-temperature emission, of $^3\text{MLCT}$ nature as it happens for this type of complexes, falls in the high-energy region of the visible range (Table 3). In particular, for $[\text{Re}(\text{2})(\text{py})(\text{CO})_3]^+$ the emission maximum, λ_{em} , falls at higher energy than for $[\text{Re}(\text{3})(\text{py})(\text{CO})_3]^+$ (Fig. 8 and Table 3). In the latter case, the presence of a more delocalised ligand appears to be a stabilizing factor. It is also to be noted that $[\text{Re}(\text{3})(\text{py})(\text{CO})_3]^+$ is easier to oxidize than $[\text{Re}(\text{2})(\text{py})(\text{CO})_3]^+$ ($E_{1/2}^{\text{ox}} = +1.75$ vs. $+1.93$ V respectively, Table 1). For both complexes, the luminescence lifetimes are shorter than 1 ns (Table 3) and all of this is consistent with a room-temperature $^3\text{Re} \rightarrow \text{L}$ CT emission.^{27–29}

Previous reports on the luminescence of Re(I) complexes indicated that their $^3\text{MLCT}$ luminescent level can be strongly destabilized at 77 K, where the solvent is frozen. The blue-shift of the $^3\text{MLCT}$ energy level can be as high as 2700 cm^{-1} .²⁸ At odds with expectations, for both $[\text{Re}(\text{2})(\text{py})(\text{CO})_3]^+$ and $[\text{Re}(\text{3})(\text{py})(\text{CO})_3]^+$ the emission spectra at 77 K are well resolved, peak at very close values ($\lambda_{\text{em}} = 572$ and 577 nm respectively), and are red-shifted by ~ 3800 and 1500 cm^{-1} respectively, with respect to what happens at room temperature (Table 3 and Fig. 8). In addition, time-resolved determinations reveal that these emissions have lifetimes of 1.5 and 1.6 ms respectively. All of this suggests that the expected displacement to high energy of the $^3\text{MLCT}$ levels unveils the presence of ^3LC levels.²⁷ These levels are centered on the coordinated bisquinoline ligands **2** and **3**, for $[\text{Re}(\text{2})(\text{py})(\text{CO})_3]^+$ and $[\text{Re}(\text{3})(\text{py})(\text{CO})_3]^+$ respectively, and are responsible for the detected emission.

At room temperature, the ruthenium series shows some peculiar properties with respect to what is commonly observed in the vast family of Ru(II)–polyimine complexes.^{10,14,15} To begin with, the emission of $[\text{Ru}(\text{1})(\text{phen})_2]^{2+}$ is blue-shifted, $\lambda_{\text{em}} = 586$ nm, and its quantum yield is $\phi_{\text{em}} = 0.0075$ (Table 3), less than half that of $[\text{Ru}(\text{phen})_3]^{2+}$ ($\lambda_{\text{em}} = 604$ nm, $\phi_{\text{em}} = 0.02$).^{14,32} A similar trend in the emission energy is apparent for $[\text{Ru}(\text{2})_3]^{2+}$ and $[\text{Ru}(\text{3})_3]^{2+}$, with $\lambda_{\text{em}} = 566$ nm in both cases, *i.e.* further blue-shifted with respect to what happens for $[\text{Ru}(\text{1})(\text{phen})_2]^{2+}$. In addition, the spectral profiles for $[\text{Ru}(\text{2})_3]^{2+}$ and $[\text{Ru}(\text{3})_3]^{2+}$ appear narrower than that for $[\text{Ru}(\text{1})(\text{phen})_2]^{2+}$ (see Fig. 7, room-temperature case, upper panel). The lifetime of these complexes is $\sim 0.9\text{ }\mu\text{s}$ (Table 3), as for $[\text{Ru}(\text{phen})_3]^{2+}$ and $[\text{Ru}(\text{bpy})_3]^{2+}$.¹⁴ Interestingly, for $[\text{Ru}(\text{2})_3]^{2+}$ and $[\text{Ru}(\text{3})_3]^{2+}$ the radiative rate constant, $k_r \sim 2\text{--}3 \times 10^3\text{ s}^{-1}$, is much lower than that for the $^3\text{MLCT}$ emitters $[\text{Ru}(\text{phen})_3]^{2+}$ or $[\text{Ru}(\text{bpy})_3]^{2+}$, $k_r \sim 8 \times 10^4\text{ s}^{-1}$.³³ In conclusion, all of this suggests a LC contribution to the room-temperature emission for $[\text{Ru}(\text{1})(\text{phen})_2]^{2+}$, $[\text{Ru}(\text{2})_3]^{2+}$ and $[\text{Ru}(\text{3})_3]^{2+}$. In fact, for the closely related $[\text{Ru}(\text{i-biq})_3]^{2+}$ species, the LC nature of the emission has been since long established.¹⁵

Low-temperature results for these Ru(II) complexes support a predominant LC nature for the emission, Table 3 and Fig. 7. This conclusion is based on the observations that (i) only for $[\text{Ru}(\text{1})(\text{phen})_2]^{2+}$ is a small blue-shift of emission peak (5 nm) observed upon passing from room temperature to 77 K; instead, a red-shift for the peak (15 nm) is registered for $[\text{Ru}(\text{2})_3]^{2+}$ and $[\text{Ru}(\text{3})_3]^{2+}$, (ii) for $[\text{Ru}(\text{1})(\text{phen})_2]^{2+}$, $[\text{Ru}(\text{2})_3]^{2+}$, and $[\text{Ru}(\text{3})_3]^{2+}$, the 77 K emission spectra peak at the same value, $\lambda_{\text{em}} = 581$ nm, (iii) the emission profiles at 77 K are narrow and well resolved for all the three complexes. While these data support an LC nature

for the emission properties at 77 K, it remains to be said that the lifetime values are typical of a ³MLCT emission, $\tau = 4.6$ – $5.2 \mu\text{s}$, Table 3. This apparent discrepancy might be the result of a complex interplay of excited states, an occurrence sometimes met for closely lying LC and MLCT levels.^{34–38}

Conclusions

Substituted 3,3'-biisoquinolines have virtually never been used in coordination photochemistry. In the present study we have made and studied transition-metal complexes of various 8,8'-disubstituted-3,3'-biisoquinolines, the two substituents attached on the 8 and 8' positions of the ligand being Cl atoms, *p*-anisyl groups or *p*-(4'-methoxy-1,1'-biphenyl) substituents. The general shape of the chelating unit is such that, although its coordination site is endotopic, *i.e.* directed towards the concave part of the molecule, it does not interfere from a steric viewpoint with the complexed metal and its close surrounding, or only very weakly. The complexes containing the Fe(II), Ru(II) or Re(I) centres and these endotopic, sterically non-hindering, U-shaped ligands have been characterized from a photophysical viewpoint. For all of the complexes the lowest-energy absorption band is of ¹MLCT nature. The emission properties of the Ru(II) and Re(I) complexes show some peculiar features: the emission of the Ru(II) complexes is of mixed ³MLCT/³LC character both at room temperature and at 77 K, whereas the emission of the Re(I) complexes appears to be of ³MLCT character at room temperature and of ³LC character at 77 K.

Acknowledgements

We thank CNR of Italy (PM P04.010) and CNRS of France. F. D. thanks the CNRS and the Région Alsace for a fellowship and O. W. acknowledges a fellowship from the Swiss National Science Foundation.

References

- 1 V. Balzani and F. Scandola, *Supramolecular Photochemistry*, Horwood, Chichester, 1991, and references therein.
- 2 V. Balzani, G. Bergamini, F. Marchioni and P. Ceroni, *Coord. Chem. Rev.*, 2006, **250**, 1254.
- 3 D. G. Cuttall, S. M. Kuang, P. E. Fanwick, D. R. McMillin and R. A. Walton, *J. Am. Chem. Soc.*, 2002, **124**, 6.
- 4 M. H. Wilson, L. P. Ledwaba, J. S. Field and D. R. McMillin, *Dalton Trans.*, 2005, 2754.
- 5 J. H. Alstrum-Acevedo, M. K. Brennaman and T. J. Meyer, *Inorg. Chem.*, 2005, **44**, 6802.
- 6 A. Hagfeldt and M. Graetzel, *Acc. Chem. Res.*, 2000, **33**, 269.

- 7 M. Hissler, J. E. McGarrah, W. B. Connick, D. K. Geiger, S. D. Cummings and R. Eisenberg, *Coord. Chem. Rev.*, 2000, **208**, 115.
- 8 O. Johansson, H. Wolpher, M. Borgstrom, L. Hammarstrom, J. Bergquist, L. C. Sun and B. Akermark, *Chem. Commun.*, 2004, 194.
- 9 P. W. Du, J. Schneider, P. Jarosz and R. Eisenberg, *J. Am. Chem. Soc.*, 2006, **128**, 7726.
- 10 A. Juris, F. Barigelletti, V. Balzani, P. Belser and A. von Zelewsky, *Inorg. Chem.*, 1985, **24**, 202.
- 11 F. Barigelletti, A. Juris, V. Balzani, P. Belser and A. von Zelewsky, *Inorg. Chem.*, 1987, **26**, 4115.
- 12 M. Kato, K. Sasano, C. Kosuge, M. Yamazaki, S. Yano and M. Kimura, *Inorg. Chem.*, 1996, **35**, 116.
- 13 M. I. Azocar, L. Mikelsons, G. Ferraudi, S. Moya, J. Guerrero, P. Aguirre and C. Martinez, *Organometallics*, 2004, **23**, 5967.
- 14 A. Juris, V. Balzani, F. Barigelletti, S. Campagna, P. Belser and A. von Zelewsky, *Coord. Chem. Rev.*, 1988, **84**, 85.
- 15 P. Belser, A. von Zelewsky, A. Juris, F. Barigelletti, A. Tucci and V. Balzani, *Chem. Phys. Lett.*, 1982, **89**, 101.
- 16 F. Duroola, J. P. Sauvage and O. S. Wenger, *Chem. Commun.*, 2006, 171.
- 17 F. Duroola, D. Hanss, P. Roesel, J. P. Sauvage and O. S. Wenger, *Eur. J. Org. Chem.*, 2007, 125.
- 18 F. Duroola, L. Russo, J.-P. Sauvage, K. Rissanen and O. S. Wenger, *Chem.–Eur. J.*, 2007, **13**, 8749.
- 19 J. N. Demas and G. A. Crosby, *J. Phys. Chem.*, 1971, **75**, 991.
- 20 D. F. Eaton, *Pure Appl. Chem.*, 1988, **60**, 1107.
- 21 K. Nakamaru, *Bull. Chem. Soc. Jpn.*, 1982, **55**, 2967.
- 22 H. Fukumi and H. Kurihara, *Heterocycles*, 1978, **9**, 1197.
- 23 D. Collado, E. Perez-Inestrosa and R. Suau, *J. Org. Chem.*, 2003, **68**, 3574.
- 24 N. Kang, A. R. Hlil and A. S. Hay, *J. Polym. Sci., Part A: Polym. Chem.*, 2004, **42**, 5745.
- 25 P. S. Braterman, J. I. Song and R. D. Peacock, *Inorg. Chem.*, 1992, **31**, 555.
- 26 C. Hamann, A. Von Zelewsky, A. Neels and H. Stoeckli-Evans, *Dalton Trans.*, 2004, 402.
- 27 K. S. Schanze, D. B. Macqueen, T. A. Perkins and L. A. Cabana, *Coord. Chem. Rev.*, 1993, **122**, 63.
- 28 D. A. Bardwell, F. Barigelletti, R. L. Cleary, L. Flamigni, M. Guardigli, J. C. Jeffery and M. D. Ward, *Inorg. Chem.*, 1995, **34**, 2438.
- 29 L. A. Worl, R. Duesing, P. Y. Chen, L. Dellaciana and T. J. Meyer, *J. Chem. Soc., Dalton Trans.*, 1991, 849.
- 30 M. Montalti, A. Credi, L. Prodi and M. T. Gandolfi, *Handbook of Photochemistry*, Taylor and Francis, Boca Raton, 2006.
- 31 A. Gilbert and J. Baggot, *Essentials of Molecular Photochemistry*, Blackwell, London, 1991.
- 32 Y. Kawanishi, N. Kitamura and S. Tazuke, *Inorg. Chem.*, 1989, **28**, 2968.
- 33 G. H. Allen, R. P. White, D. P. Rillema and T. J. Meyer, *J. Am. Chem. Soc.*, 1984, **106**, 2613.
- 34 D. S. Tyson and F. N. Castellano, *J. Phys. Chem. A*, 1999, **103**, 10955.
- 35 N. D. McClenaghan, F. Barigelletti, B. Maubert and S. Campagna, *Chem. Commun.*, 2002, 602.
- 36 A. F. Morales, G. Accorsi, N. Armaroli, F. Barigelletti, S. J. A. Pope and M. D. Ward, *Inorg. Chem.*, 2002, **41**, 6711.
- 37 X. Y. Wang, A. Del Guerso and R. H. Schmehl, *J. Photochem. Photobiol., C*, 2004, **5**, 55.
- 38 N. D. McClenaghan, Y. Leydet, B. Maubert, M. T. Indelli and S. Campagna, *Coord. Chem. Rev.*, 2005, **249**, 1336.